

DOIhttps://doi.org/10.1007/s11595-019-2191-y

# Microstructure, Texture, and Hardness Evolutions of Al-Mg-Si-Cu Alloy during Annealing Treatment

WANG Xiaofeng<sup>1</sup>, MA Cunqiang<sup>2</sup>, MA Pengcheng<sup>3</sup>, ZHOU Songze<sup>1</sup>, WANG Yonggang<sup>1</sup>

(1. Key Laboratory of Impact and Safety Engineering (Ningbo University), Ministry of Education, Ningbo 315211, China; 2. Capital Aerospace Machinery Company, Beijing 100076, China; 3. Aerospace Research Institute of Materials and Processing Technology, Beijing 100076, China)

**Abstract:** Microstructure, texture and hardness evolutions of Al-Mg-Si-Cu alloy during annealing treatment were studied by microstructure, texture and hardness characterization in the present study. The experimental results show that microstructure, texture and hardness will change to some extent with the increase of annealing temperature. The microstructure transforms from the elongated bands to elongated grains first, and then the grains grow continuously. The texture transforms from the initial deformation texture  $\beta$  fiber to recrystallization texture mainly consisting of  $\text{Cube}_{\text{ND}} \{001\} \langle 310 \rangle$  and  $\text{P} \{011\} \langle 122 \rangle$  orientations first, and then the recrystallization texture may be enhanced continuously as a result of the grain growth. Hardness decreases slowly at first, and then decreases sharply and increases significantly finally. Besides, the particle distributions also have great changes. As the annealing temperature increases, they increase firstly as a result of precipitation, and then gradually disappear as a result of dissolution. Finally, the effect of annealing temperature on microstructure, texture and hardness evolutions is discussed.

**Key words:** Al-Mg-Si-Cu alloy; hardness; microstructure; texture; recrystallization

## 1 Introduction

Recently, age hardenable Al-Mg-Si-Cu alloys have received considerable attention in auto body outer panels due to their advantages of high strength-to-weight ratio, sufficient formability and good corrosion resistance<sup>[1-3]</sup>. The typical fabrication processing of Al-Mg-Si-Cu alloy sheets consists of casting, homogenization, hot rolling, intermediate annealing, cold rolling and solution treatment<sup>[4,5]</sup>. Finally, the Al-Mg-Si-Cu alloy sheets are always subjected to some aging treatments for the final application. As the fabrication processing is long and complicated, many factors such as rolling parameter, intermediate annealing parameter and solution treatment parameter may significantly affect their microstructure and texture, thus influencing the final mechanical property<sup>[6-9]</sup>. Therefore, it has been the extensive

research subject. Obviously, annealing treatment plays a critical role in the microstructure and texture development of Al-Mg-Si-Cu alloy. It is experimental proven<sup>[7,9]</sup> that with increasing the annealing temperature and time, the aspect ratio of the elongated grains gradually decreases. In addition, although the intermediate annealing temperature and time could affect the final recrystallization texture, their effect on intermediate annealing texture was not yet investigated.

In general, when the deformed Al-Mg-Si-Cu alloys are subjected to the annealing treatment, they may experience two stages: recovery and recrystallization<sup>[10-12]</sup>. Recovery is primarily due to changes in the dislocation structure, and the microstructural and textural changes are very slight in the recovery stage of low temperature. In the recrystallization stage of high temperature, the recrystallization process may involve nucleation and grain growth, thus the microstructure and texture could take place great changes. Furthermore, considering the Al-Mg-Si-Cu alloy is a precipitable strengthening alloy, the precipitation and dissolution could be occurred during the annealing treatment, depending on the annealing temperature. And the particles can significantly influence the microstructure and texture according to their effect on recrystallization progressing<sup>[13]</sup>. Accordingly, the microstructure and texture evolutions are very complicated, and thus

© Wuhan University of Technology and Springer-Verlag GmbH Germany, Part of Springer Nature 2019

(Received: Oct. 18, 2018; Accepted: Jan. 10, 2019)

WANG Xiaofeng (汪小锋): Lecturer; Ph D; E-mail: wangxiaofeng@nbu.edu.cn

Funded by the Science Challenge Project (No.TZ2018001), the Zhejiang Provincial Natural Science Foundation of China (No. LQ17E010001), the Ningbo Natural Science Foundation (No.2018A610174), the Natural Science Foundation of Ningbo University (No. XYL18017) and the KC Wong Magna Fund from Ningbo University

resulting in a complicated hardness variation. Presently, there is still no systematic study on the microstructure and texture evolution of Al-Mg-Si-Cu alloy during the annealing treatment, which is very critical for the development of final microstructure and texture due to the genetic character of microstructure and texture evolutions. Additionally, the hardness evolution also needs to be understood. Accordingly, the aim of the present study is to understand the microstructure, texture and hardness evolutions of Al-Mg-Si-Cu alloy during the annealing treatment, and hopefully clarify the related the evolve mechanism, thus providing a guide to choose a reasonable annealing parameter.

## 2 Experimental

The starting material was a cold-rolled Al-Mg-Si-Cu alloy sheet with a thickness of 1 mm and a chemical composition of Al-0.7Mg-0.9Si-0.7Cu-0.3Fe-0.2Mn (wt%). To investigate the microstructure, texture and hardness evolutions during the annealing treatment, the sheet was divided into several parts and they were heated from room temperature to different temperatures (100 °C, 150 °C, 200 °C, 250 °C, 300 °C, 350 °C, 400 °C, 450 °C, 500 °C, and 550 °C) in an air furnace at a heating rate of 20 °C/h. After that, in order to maintain the microstructure and texture of current state, the annealed parts were quenched in water immediately.

Vickers micro-hardness measurements were carried out on the longitudinal sections of the initial and annealed specimens using a Wolpert-401MVD Vickers hardness tester under a load of 200 g for the holding time of 30 s. In order to ensure the accuracy of data, one valid testing data was acquired for repeating ten times.

Microstructure was observed by a Carl ZEISS Axio Imager A2m optical microscope. The samples were ground and polished according to standard metallographical techniques, and then etched using Keller's reagent (95 mL H<sub>2</sub>O+2.5 mL HNO<sub>3</sub>+1.5 mL HCL+1 mL HF).

The particle distributions in the alloy matrix were investigated using the Hitachi SU 5000 scanning electron microscope (SEM) equipped with X-ray energy dispersive spectrometers (EDS) systems and Tecnaig2 F30 transmission electron microscope (TEM). Samples for SEM observation were prepared according to the standard metallographical techniques. Samples for TEM observation were mechanically ground on both surfaces to approximately 100 mm and then twin-jet polished in an electrolyte containing

30vol% nitric acid and 70vol% methanol at -25 °C.

The microstructure and texture evolutions during the annealing treatment were characterized on a Hitachi SU 5000 scanning electron microscope equipped with an Oxford Instruments AZtec HKL electron-backscatter diffraction (EBSD) system. EBSD samples were prepared by grinding, mechanical polishing and electro-polishing with a solution of 6% perchloric acid and 94% ethanol at -20 °C. The EBSD results were analyzed using the HKL Channel 5 software. Orientation distribution functions (ODFs) were calculated using the harmonic series expansion method (orthorhombic sample symmetry,  $l_{\max}=22$ , Gaussian spread=5°). The ODFs were represented as plots of constant  $\phi_2$  sections with iso-intensity contours in Euler space defined by the Euler angles  $\phi_1$ ,  $\Phi$ , and  $\phi_2$ . During the misorientation statistics calculation, grain boundaries with a misorientation of < 2° was neglected as a result of the inaccuracy. For the recrystallization fraction calculation in Tango, the minimum misorientation angle to define a subgrain was set as 2° and the minimum misorientation angle to define a grain was set as 10°.

The initial macro-texture was measured at one quarter the thickness of the cold-rolled Al-Mg-Si-Cu alloy sheet. A sample with dimensions of 20 mm (rolling direction)×15 mm (transverse direction) was prepared for pole figure measurement. The three pole figures consisting of (111), (200), and (220) were measured using the Schulz back-reflection method on a Panalytical X'pert MRD X-ray diffractometer equipped with a Co radiation source. The ODFs and the specific texture volume fractions were calculated by the JTEX software.

## 3 Results

### 3.1 Hardness evolution of the cold-rolled Al-Mg-Si-Cu alloy sheet

Fig.1 presents Vickers hardness of the specimens annealed at different temperatures. As can be seen, the hardness decreases slowly at first, and then decreases sharply, and finally increases significantly. Obviously, the interesting hardness-temperature curve may have a close correlation with the recrystallization progress and secondary phase particles. The hardness could be reflected by the microstructure, and low temperature is difficult to change microstructure and texture, accordingly, four specimens at the typical annealing temperatures (300 °C, 400 °C, 500 °C, and 550 °C) were selected to investigate their microstructure and textures.

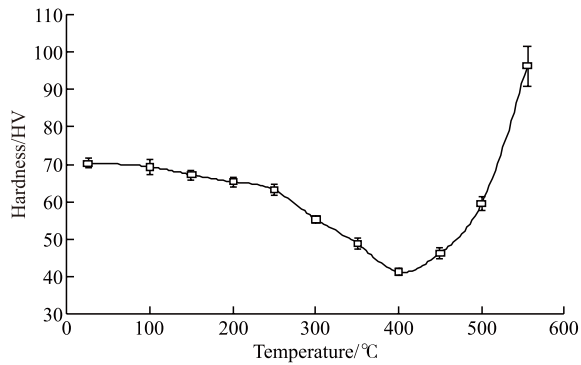


Fig.1 Vickers hardness of the Al-Mg-Si-Cu alloy at different temperatures during the annealing treatment

### 3.2 Microstructure evolution of the cold-rolled Al-Mg-Si-Cu alloy sheet

Fig.2 shows the microstructure and particle

distributions of the starting cold-rolled Al-Mg-Si-Cu alloy sheet. It exhibits typical deformed structure consisting of a large number of parallel elongated bands along the rolling direction (as shown in Fig.2(a)). Four types of particles with different colors and shapes could be found in the alloy matrix (as shown in Fig.2(b)). According to EDS analysis (as shown in Figs.2(c-f)), the large white particles exceeding 1  $\mu\text{m}$  are confirmed as Al(Fe,Mn)Si, the black particles are confirmed as  $\text{Mg}_2\text{Si}$ , the gray particles are confirmed as Si, and the fine dark white particles are confirmed as Q ( $\text{Al}_{1.9}\text{Mg}_{4.1}\text{Si}_{3.3}\text{Cu}$ ). In addition, the previous study<sup>[7]</sup> has revealed that there are also some white fine Al(Fe,Mn)Si particles in the alloy matrix besides the coarse Al(Fe,Mn)Si particles. They should be developed by breaking of the coarse Al(Fe,Mn)Si particles during cold rolling.

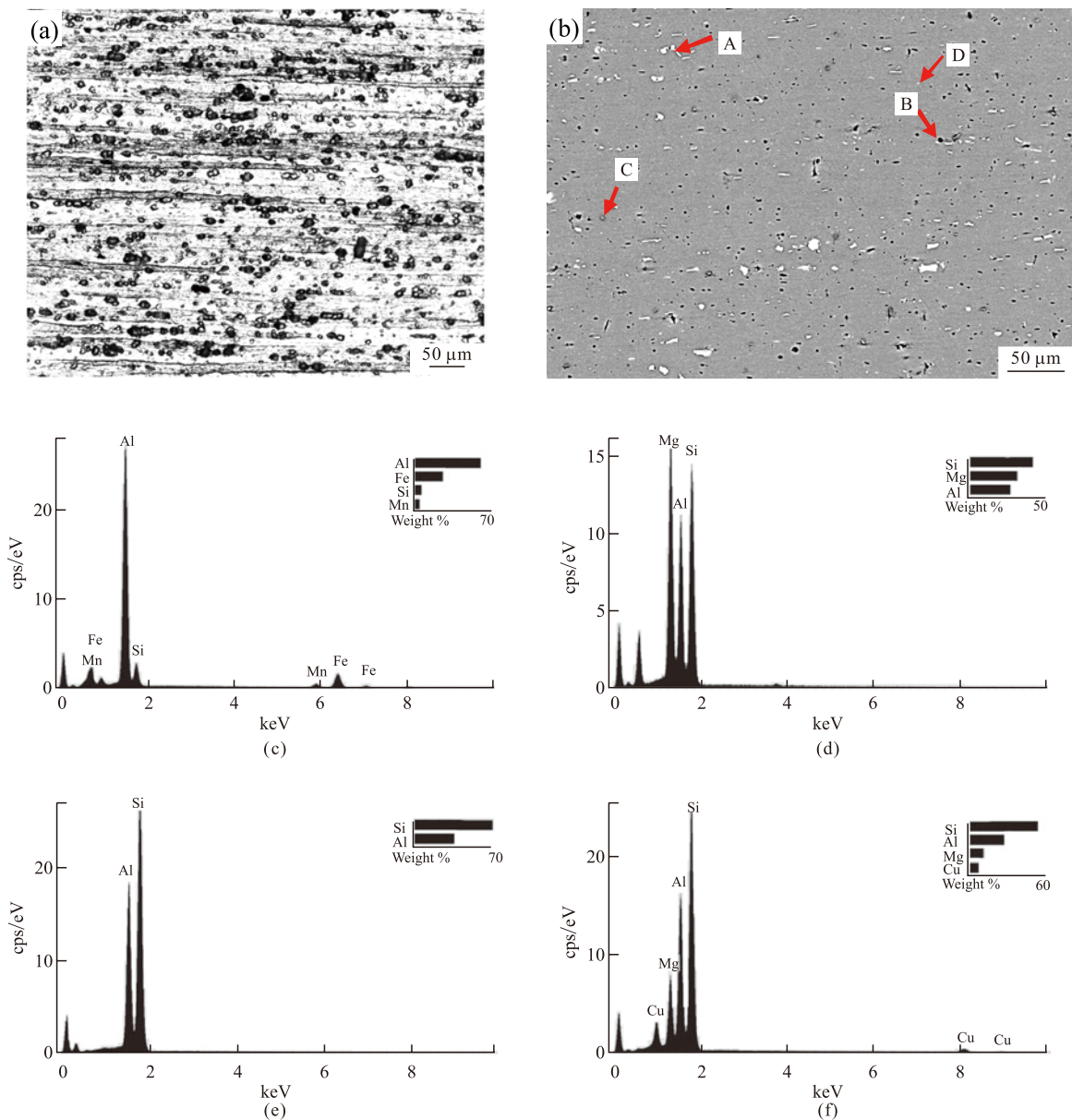


Fig.2 OM and SEM analysis on the cold-rolled Al-Mg-Si-Cu alloy sheet: (a) microstructure, (b) particle distribution, and (c-f) EDS spectra of the particles

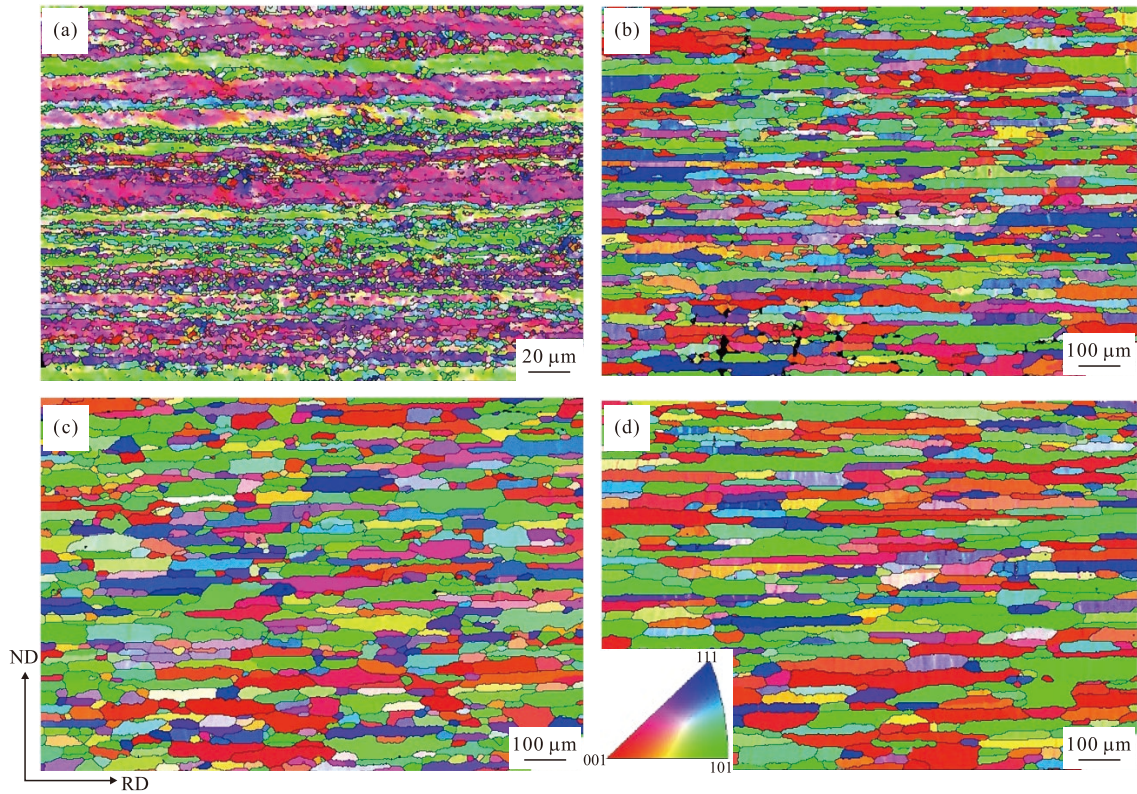


Fig.3 IPF maps of the cold-rolled Al-Mg-Si-Cu alloy sheet during the annealing treatment: (a) 300 °C, (b) 400 °C, (c) 500 °C, and (d) 555 °C

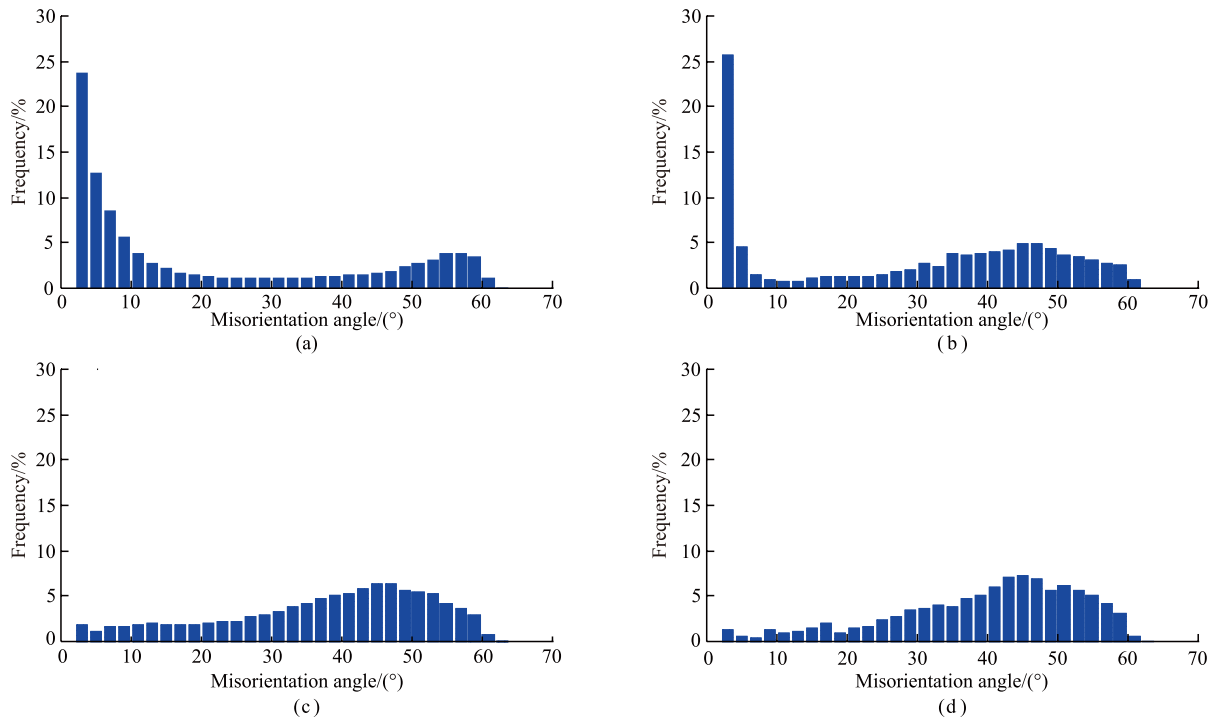


Fig.4 Misorientation angle distributions of the cold-rolled Al-Mg-Si-Cu alloy sheet during the annealing treatment: (a) 300 °C, (b) 400 °C, and (c) 500 °C, (d) 555 °C

Fig.3 reveals the microstructure evolution of the cold-rolled Al-Mg-Si-Cu alloy sheet during the annealing treatment. It could be found that the microstructure took place great changes with the increase of the annealing temperature. As the

annealing temperature rises, the microstructure transformed from the elongated bands to the elongated grains. The microstructure at 300 °C includes lots of elongated bands and some very fine deformed grains, implying that recovery is dominant in this stage. All

the microstructure at 400 °C, 500 °C, and 555 °C is mainly comprised of the elongated grains. Notably, the fine deformed grains gradually decrease with the increase of annealing temperature, indicating that the fine grains were gradually replaced by the elongated recrystallization grains. Additionally, the elongated grains become coarse, with rising the annealing temperature. This is attributable to the long holding time and high temperature during the annealing treatment. Fig.4 presents the misorientation angle distributions of the Al-Mg-Si-Cu alloy sheet during the annealing treatment. It could be seen that as the annealing temperature rises, the low angle grain boundaries (LAGB) gradually decrease and high angle grain boundaries (HAGB) gradually increase, indicating that a large number of deformation substructure disappears and recrystallization microstructure is dominant. According to Channel 5 software, the recrystallization fractions of the Al-Mg-Si-Cu alloy sheet during the annealing treatment could be obtained. The recrystallization fractions of the sheets at 300 °C, 400 °C, 500 °C, and 550 °C are 9.7%, 47.3%, 86.9%, and 94.3%, respectively. It is clear that as the annealing temperature rises, the recrystallization fraction firstly increases, and then almost remains constant.

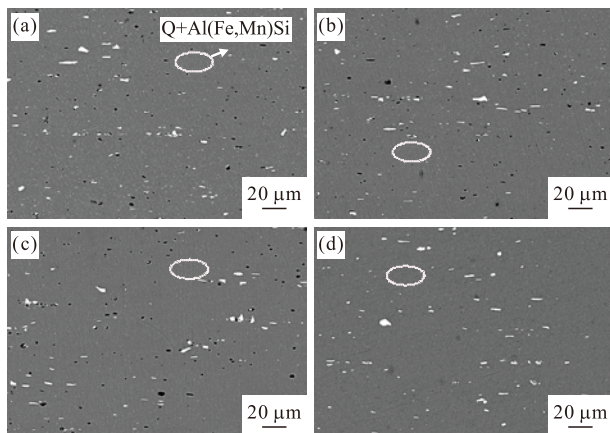


Fig.5 Particle distributions of the cold-rolled Al-Mg-Si-Cu alloy sheet during the annealing treatment: (a) 300 °C, (b) 400 °C, (c) 500 °C, and (d) 555 °C

During the annealing treatment, the particle distribution may change a lot due to the precipitation and dissolution of the particles. The particle distributions are presented in Fig.5. There are many particles in the alloy matrix. According to the colors and shapes of the particles, it can be inferred that the particle types could be kept unchanged during the annealing treatment. Therefore, Al(Fe,Mn)Si, Mg<sub>2</sub>Si, Si, and Q are still the main particles. It is worth noting that the fine white particles are Al(Fe,Mn)Si and Q. As the annealing temperature rises, the fine white particles

gradually decrease. When the annealing temperature reaches 555 °C, only the white particles of Al(Fe,Mn)Si distribute in the alloy matrix, indicating that almost all the soluble particles such as Mg<sub>2</sub>Si, Si, and Q could be dissolved completely. In order to investigate the particle distributions more clearly, TEM observations for the particle distributions of the Al-Mg-Si-Cu alloy sheet during the annealing treatment are shown in Fig.6. Some dislocation network can be observed when the annealing temperature is 300 °C, indicating that the microstructure still includes some deformation substructure. As the annealing temperature rises, the dislocations gradually disappear and the particles increase at first, and then gradually decrease.

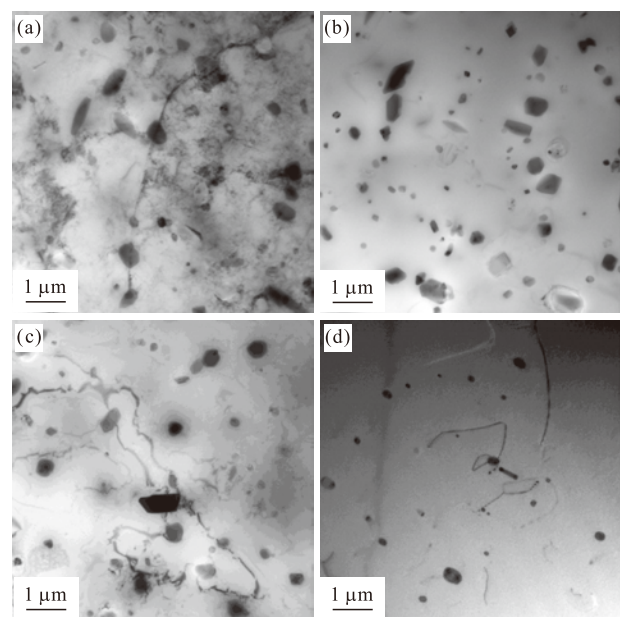


Fig.6 TEM micrographs of the cold-rolled Al-Mg-Si-Cu alloy sheet during the annealing treatment: (a) 300 °C, (b) 400 °C, (c) 500 °C, and (d) 555 °C

### 3.3 Texture evolution of the cold-rolled Al-Mg-Si-Cu alloy sheet

The cold rolling texture of the Al-Mg-Si-Cu alloy sheet is presented in Fig.7. It reveals a strong  $\beta$  fiber, mainly including Copper  $\{112\}\langle 111\rangle$ , S  $\{123\}\langle 634\rangle$  and Brass  $\{011\}\langle 211\rangle$  orientations with intensities of 7.0, 11.3, and 10.6, respectively. Their corresponding volume fractions are 8.7%, 11.8%, and 12.8%, respectively. Additionally, Goss  $\{110\}\langle 001\rangle$  orientation with an intensity of 6.6 can also be found, and its volume fraction is 4.4%.

The above microstructure evolution results suggest that microstructure of the Al-Mg-Si-Cu alloy sheet could take place great changes during the annealing treatment. Obviously, the texture may also transform continuously during the annealing treatment. The through-thickness annealing textures

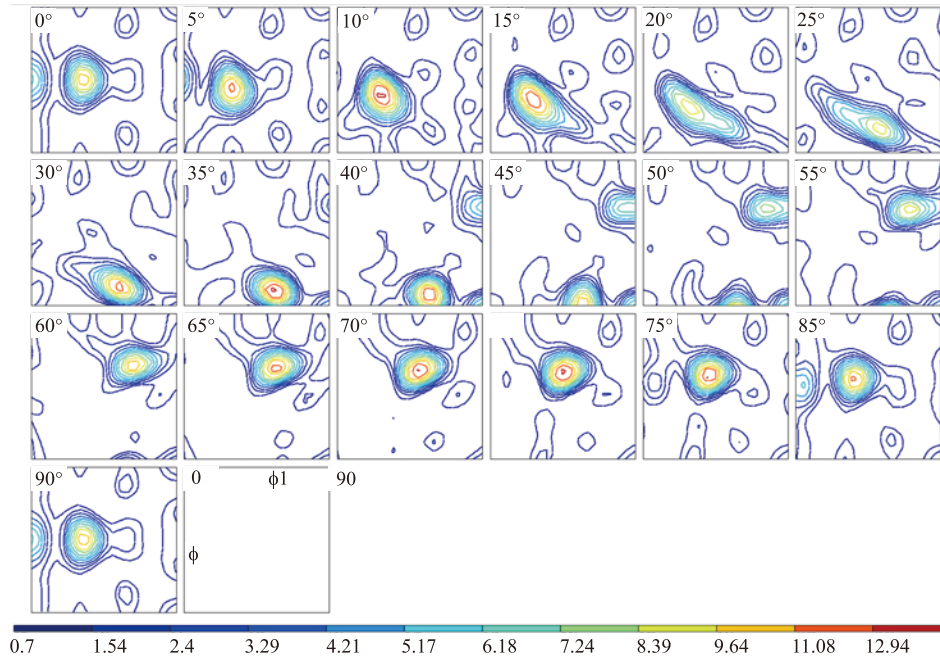


Fig.7 Texture of the cold-rolled Al-Mg-Si-Cu alloy sheet

**Table 1** The volume fractions of texture components of the cold-rolled Al-Mg-Si-Cu alloy sheet during the annealing treatment

Annealing time	Texture component	Intensity	Volume fraction/%
300 °C	{023}<532>	7.7	14.3
	Copper	19.2	25.5
	S	16.1	45.5
400 °C	Cube <sub>ND</sub>	4.5	12.8
	P	6.8	14.4
	Cube <sub>ND</sub>	4.0	10.2
500 °C	P	6.8	19.2
	Goss	3.0	4.1
	Cube <sub>ND</sub>	5.6	16.7
555 °C	P	8.5	22.5
	Goss	3.0	2.7

of the Al-Mg-Si-Cu alloy sheet during the annealing treatment are presented in Fig.8. It is evident that their textures are significantly influenced by the annealing temperature. When the annealing temperature rises from room temperature to 300 °C, the texture is similar to the initial cold rolling texture, and the main texture components are Copper and S orientations. Additionally, a strange texture component {023}<532> similar to Brass component could be found, indicating that Brass component has transformed to {023}<532> component as a result of the local recrystallization. When the annealing temperature rises to 400 °C, all the deformation texture is completely replaced

by recrystallization texture including Cube<sub>ND</sub> {001}<310> and P {011}<122> orientations. When the annealing temperature reaches 500 and 555 °C, their recrystallization textures are similar, and Cube<sub>ND</sub>, P, and Goss orientations are the main texture components. The intensities and volume fractions of the specific texture components are summarized in Table 1. It can be reflected that as the annealing temperature rises, on one hand, the texture gradually transforms from the deformation texture to recrystallization texture, on the other hand, the recrystallization texture could be kept unchanged and gradually becomes strong, indicating the grains possess an excellent stability. The above recrystallization texture components Cube<sub>ND</sub> and P have been reported in other studies<sup>[14,15]</sup> and they are well reflected that particle stimulated nucleation (PSN) is the main recrystallization mechanism. Additionally, Goss orientation could be attributed to the recrystallization nucleation at shear bands.

## 4 Discussion

### 4.1 Effect of annealing temperature on the hardness

As previously depicted, the variation of hardness with annealing temperature is very interesting. During the temperature rising stage, recovery, recrystallization, precipitation and dissolution may occur concurrently. Fang *et al*<sup>[16]</sup> have confirmed that equilibrium Mg<sub>2</sub>Si could precipitate at 400 °C according to differential scanning calorimetry (DSC) analysis. Miao *et al*<sup>[17]</sup> also

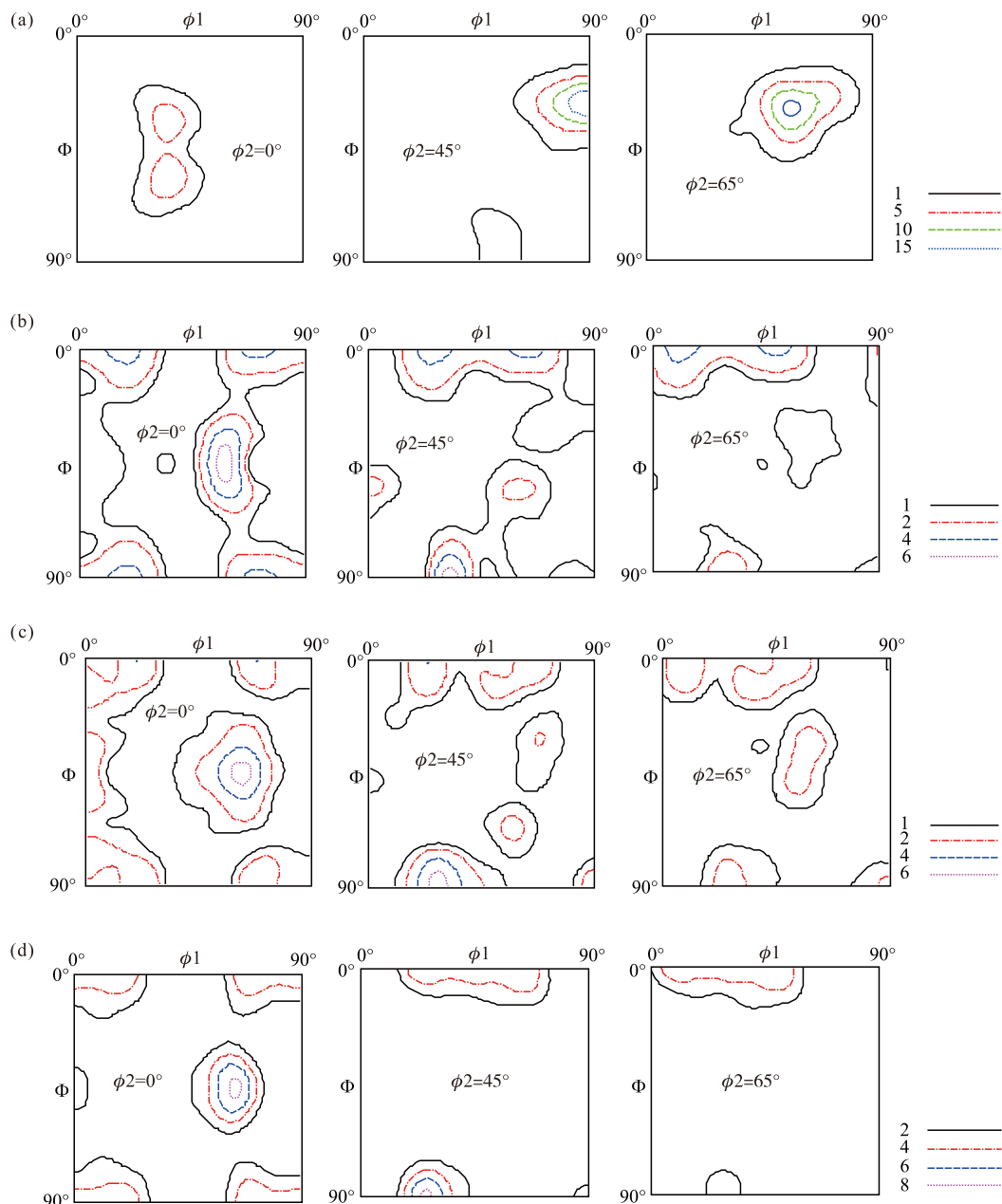


Fig.8 Texture evolution of the cold-rolled Al-Mg-Si-Cu alloy sheet during the annealing treatment: (a) 300 °C, (b) 400 °C, (c) 500 °C, and (d) 555 °C

obtained the similar experimental results that the precipitation peak of  $Mg_2Si$  and Si is at 400 °C and their dissolution peak is at about 500 °C. Esmaeili *et al*<sup>[18]</sup> studied the precipitation behavior of the AA6111 alloy and pointed out that the precipitation peak of Q is about 345 °C. However, the alloy elements of the present Al-Mg-Si-Cu alloy are somewhat different from those of the above mentioned alloys. Consequently, the precipitation and dissolution temperatures in the present alloy may have slight deviation from those in the previously mentioned studies. The phase diagram could provide some information about precipitation and dissolution. Fig.9 presents equilibrium phase diagram of Al-Mg-Si-

Cu alloys with different contents of Cu (0 to 2wt%). It can be found that as the temperature rises, the phase may take place some changes. When the temperature is in the range of 220-360 °C,  $Al_2Cu$  vanishes; when the temperature is in the range of 360-420 °C,  $Mg_2Si$  particles start to appear; when the temperature is in the range of 420-480 °C, Q particles disappear; when the temperature is in the range of 480-550 °C, Si particles disappear; when the temperature exceeds 550 °C,  $Mg_2Si$  particles disappear. Accordingly, the precipitation and dissolution occur during the temperature rising stage. Since no  $Al_2Cu$  could be found in the initial alloy, it could be approximately considered that almost

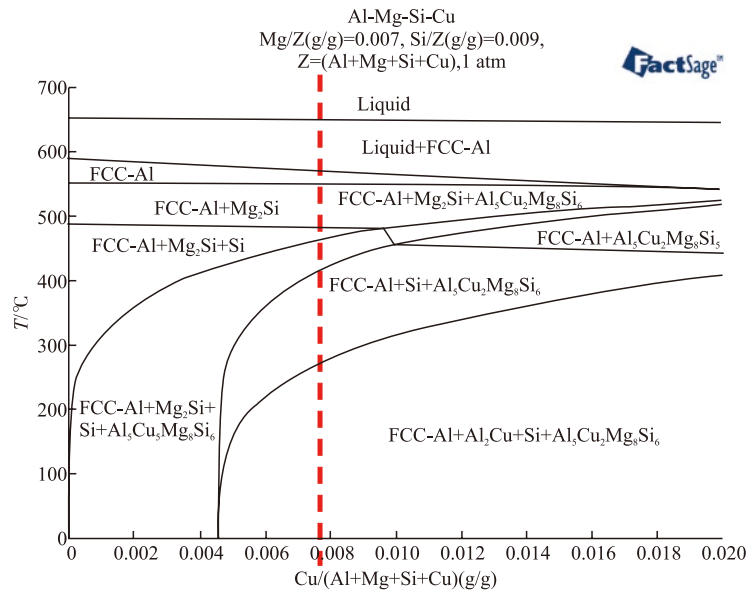


Fig.9 Equilibrium phase diagram of alloys with different contents of Cu (0 to 2wt%) calculated using FactSage software

no precipitation and dissolution could take place before 360 °C.

The combined effect of recovery, recrystallization, precipitation and dissolution may result in the variation of hardness. The hardness decreases slowly until the temperature reaches 250 °C, indicating that the recovery is dominant in the alloy before 250 °C. After that, the hardness decreases sharply, implying that recrystallization was occurred gradually. However, when the temperature exceeds 400 °C, the hardness increases significantly, and the strengthening mechanism is determined by the temperature. When the temperature is in the range of 400-450 °C, the strengthening could be attributed to the competition of precipitation and recrystallization. When the temperature exceeds 500 °C, the recrystallization is finished according to EBSD results, thus the strengthening could be attributed to the solution strengthening, which implies that solution strengthening effect exceeds precipitation strengthening effect.

#### 4.2 Effect of annealing temperature on the microstructure and texture

On the basis of the preceding microstructure and texture evolution results, it is apparent that the effect of recovery on the microstructure and texture of the Al-Mg-Si-Cu alloy sheet is really negligible, however, recrystallization progress significantly influences the microstructure and texture. Recrystallization progress may be affected by some factors such as annealing temperature, annealing time and particles. Considering annealing temperature and annealing time could affect the stored energy of deformation, recrystallization may be affected by stored energy of deformation and

particles, and the driving force for recrystallization can be expressed as<sup>[19,20]</sup> :

$$V = MP = M \cdot (P_D - P_C - P_Z) \\ = M_0 \exp(-Q/kT) \left( \frac{\alpha \rho G b^2}{2} - \frac{2\gamma_b}{R} - \frac{3F_v \gamma_b}{d_p} \right) \quad (1)$$

where,  $M$ ,  $P_D$ ,  $P_C$ , and  $P_Z$  are the mobility of grain boundaries, the stored energy of deformation, the retarding pressure due to the grain boundary curvature and the Zener drag respectively.  $Q$ ,  $T$ ,  $\rho$ ,  $G$ ,  $\gamma_b$ ,  $R$ ,  $F_v$ , and  $d_p$  represent the activation energy, the temperature, the dislocation density, the shear module, the boundary energy, the grain radius, the volume fraction and diameter of the small particles (the size of retarding recrystallization), respectively.

During the annealing treatment, the alloy sheet was heated at a heating rate of 20 °C/h. Therefore, as the annealing temperature rises, the annealing time could also increase and the stored energy should be gradually consumed. The microstructure and texture evolution can be divided into three stages: (i) Recovery stage: When the annealing temperature is relatively low, recovery is prevailed. Accordingly, similar to the starting state, the microstructure is still composed of elongated bands and the texture is mainly comprised of the typical deformation texture, as presented in Fig.3(a) and Fig.8(a). Additionally, a great number of particles can be observed. (ii) Recrystallization stage: When the annealing temperature rises to the critical value, recrystallization begins to be dominant, elongated grains gradually replace the deformation elongated bands and the typical recrystallization texture is devel-



oped (as revealed in Figs.3(b-c) and Figs.8(b-c)). In addition, lots of particles can still be observed due to the precipitation. The fine particles may give a significant retard force on the movement of grain boundaries along normal direction (ND) and much stored energy is gradually consumed during the recovery stage, thus finally resulting in the development of elongated grains not equiaxed grains. (iii) Recrystallization grain growth stage: When the annealing temperature rises to a relatively high value, the recrystallization is finished and the grains will grow continuously. In this stage, the recrystallization grain structure is still comprised of elongated grains and texture components have no change (as shown in Fig.3(d) and Fig.8(d)). Since the soluble particles are gradually dissolved, the limited number of particles may finally result in the appreciable grain growth. The appreciable grain growth also makes the oriented grains occupy a large area and the texture may become very strong. The phenomenon is similar to the observation in electrical steel that the coarse Goss oriented grains result in the strong Goss texture.

The microstructure and texture evolutions during the annealing treatment could obtain a relationship among microstructure, texture and annealing temperature. However, the final mechanical properties are determined by the final microstructure and texture. In order to obtain the optimal final microstructure and texture, the effect of annealing microstructure and texture on the final recrystallization microstructure and texture still needs to be studied systematically in future.

## 5 Conclusions

a) The variation of hardness with annealing temperature is interesting. As the annealing temperature increases, the hardness decreases slowly at first, and then decreases sharply, and increases significantly finally.

b) As the annealing temperature increases, the microstructure transforms from the elongated bands to elongated grains first, and then the grains grow continuously. Furthermore, fraction of low angle grain boundaries (LAGBs) decreases first, and then remains constant. Additionally, the particles become more and more firstly as a result of precipitation, and then gradually disappear as a result of dissolution.

c) As the annealing temperature increases, the texture transforms from the initial deformation texture  $\beta$  fiber to recrystallization texture mainly including  $\text{Cube}_{\text{ND}} \{001\} \langle 310 \rangle$  and  $\text{P} \{011\} \langle 122 \rangle$  orientations first, and then the recrystallization texture becomes stronger and stronger due to the grain growth. However,

the texture components may have no change during the grain growth stage.

d) During the annealing treatment, Al-Mg-Si-Cu alloy may experience three stages consisting of recovery stage, recrystallization stage, recrystallization grain growth stage. Microstructure and texture evolutions are well explained by the combine effect of deformation stored energy and particle finally. Hardness variation with annealing temperature is determined by the combined effect of recovery, recrystallization, precipitation and dissolution.

## References

- [1] Rowe J. *Advanced Materials in Automotive Engineering*[M]. Woodhead: Cambridge, 2012
- [2] Hirsch J. Recent Development in Aluminium for Automotive Applications[J]. *Trans. Nonferrous Met. Soc. China*, 2014, 24: 1 995-2 002
- [3] Hirsch J, Al-Samman T. Superior Light Metals by Texture Engineering: Optimized Aluminum and Magnesium Alloys for Automotive Applications[J]. *Acta Mater.*, 2013, 61: 818-843
- [4] Engler O, Hirsch J. Texture Control by Thermomechanical Processing of AA6xxx Al-Mg-Si Sheet Alloys for Automotive Applications-a Review[J]. *Mater. Sci. and Eng. A*, 2002, 336: 249-262
- [5] Wang XF, Guo MX, Cao LY, et al. Relationship among Mechanical Properties Anisotropy, Microstructure and Texture in AA6111 Alloy Sheets[J]. *J. Wuhan Univ. Technol.*, 2016, 31: 648-653
- [6] Wang XF, Guo MX, Cao LY, et al. Effect of Heating Rate on Mechanical Property, Microstructure and Texture Evolution of Al-Mg-Si-Cu Alloy during Solution Treatment[J]. *Mater. Sci. and Eng. A*, 2015,621: 8-17
- [7] Wang XF, Guo MX, Chaupis A, et al. The Dependence of Final Microstructure, Texture Evolution and Mechanical Properties of Al-Mg-Si-Cu Alloy Sheets on the Intermediate Annealing[J]. *Mater. Sci. Eng. A*, 2015, 633: 46-58
- [8] Wang XF, Guo MX, Zhang Y, et al. The Dependence of Microstructure, Texture Evolution and Mechanical Properties of Al-Mg-Si-Cu Alloy Sheet on Final Cold Rolling Deformation[J]. *J. Alloy. Compd.*, 2016, 657: 906-916
- [9] Wang XF, Guo MX, Luo JR, et al. Effect of Intermediate Annealing Time on Microstructure, Texture and Mechanical Properties of Al-Mg-Si-Cu Alloy[J]. *Mater. Charact.*, 2018, 142: 309-320
- [10] Humphreys FJ, Hatherly M. *Recrystallization and Related Annealing Phenomena*, 2nd Ed.[M]. Elsevier: Oxford, 2004
- [11] Doherty RD, Hughes DA, Humphreys FJ, et al. Current Issues in Recrystallization: A Review[J]. *Mater. Sci. and Eng. A*, 1997, 238: 219-274
- [12] Doherty RD. Recrystallization and Texture[J]. *Prog. Mater. Sci.*, 1997, 42: 39-58
- [13] Lillywhite SJ, Prangnell PB, Humphreys FJ. Interactions between Precipitation and Recrystallisation in an Al-Mg-Si Alloy[J]. *Mater. Sci. and Technol.*, 2000, 16: 1 112-1 120
- [14] Vatne HE, Benum S, Daaland O, et al. The Effect of Particles on Recrystallisation Textures and Microstructures[J]. *Text. and Microstruct.*, 1996, 13: 385-412
- [15] Vatne HE, Engler O, Nes E. Influence of Particles on Recrystallisation Textures and Microstructures of Aluminium Alloy 3103[J]. *Mater. Sci. and Technol.*, 1997, 13: 93-102
- [16] Fang X, Song M, Li K, et al. Precipitation Sequence of an Aged Al-Mg-Si Alloy[J]. *J. Min. Metall. Sect. B-Metall.*, 2010, 46: 171-180
- [17] Miao WF, Langhlin DE. Effects of Cu Content and Preaging on Precipitation Characteristics in Aluminum Alloy 6022[J]. *Metall. Mater. Trans. A*, 2000, 31: 361-371
- [18] Esmaili S, Wang X, Lloyd DJ, et al. On the Precipitation-Hardening Behavior of the Al-Mg-Si-Cu Alloy AA6111[J]. *Metall. Mater. Trans. A*, 2003, 34: 751-763
- [19] Ferry M, Jones D. High-Rate Annealing of Single-Phase and Particle-Containing Aluminium Alloys[J]. *Scripta Mater.*, 1998, 38: 177-183
- [20] Bennett TA, Petrov RH, Kestens AI. Effect of Particles on Texture Banding in an Aluminium Alloy[J]. *Scripta Mater.*, 2010, 62: 78-81